Originally published as:

Impacts of future land cover changes on atmospheric CO$_2$ and climate

Stephen Sitch,[1] Victor Brovkin, and Werner von Bloh

Potsdam Institute for Climate Impact Research, Potsdam, Germany

Detlef van Vuuren and Bas Eickhout

Netherlands Environmental Assessment Agency (RIVM/MNP), Bilthoven, Netherlands

Andrey Ganopolski

Potsdam Institute for Climate Impact Research, Potsdam, Germany

[1] Climate-carbon cycle model CLIMBER2-LPJ is run with consistent fields of future fossil fuel CO$_2$ emissions and geographically explicit land cover changes for four Special Report on Emissions Scenarios (SRES) scenarios, A1B, A2, B1, and B2. By 2100, increases in global mean temperatures range between 1.7°C (B1) and 2.7°C (A2) relative to the present day. Biogeochemical warming associated with future tropical land conversion is larger than its corresponding biogeophysical cooling effect in A2, and amplifies biogeophysical warming associated with Northern Hemisphere land abandonment in B1. In 2100, simulated atmospheric CO$_2$ ranged from 592 ppm (B1) to 957 ppm (A2). Future CO$_2$ concentrations simulated with the model are higher than previously reported for the same SRES emission scenarios, indicating the effect of future CO$_2$ emission scenarios and land cover changes may hitherto be underestimated. The maximum contribution of land cover changes to future atmospheric CO$_2$ among the four SRES scenarios represents a modest 127 ppm, or 22% in relative terms, with the remainder attributed to fossil fuel CO$_2$ emissions.

1. Introduction

[2] Over the past several centuries, human intervention has markedly impacted land surface characteristics and atmospheric composition, in particular through large-scale land conversion for cultivation and burning of fossil fuels. Between one third and one half of the land surface has been directly transformed by human action [*Vitousek et al.*, 1997]. Land cover changes impact atmospheric composition and climate via two mechanisms: biogeochemical and biogeophysical.

[3] Biogeophysical mechanisms include the effects of changes in surface roughness, transpiration, and albedo. In general, conversion of forest to agricultural land decreases surface roughness, affecting the energy and momentum balances in, and height of, the boundary layer, by reducing the ability of air to mix. Replacing forests with cultivated lands leads to an increase in surface albedo, as dark green, closed-canopy forest is replaced with low stature, less dense croplands. The difference is particularly important in the winter and spring in areas with snow cover. During these seasons, forests retain their low albedos (about 0.2 [see, e.g., *Betts and Ball*, 1997]), whereas snow-covered fields have typically much higher albedos (up to 0.8). Indeed, *Brovkin et al.* [1999] estimated the biogeophysical effect of historical deforestation during the last millennium to be a global cooling of −0.35°C, with a more pronounced regional Northern Hemisphere cooling of −0.5°C. In a recent sensitivity study, *Matthews et al.* [2003] agrees on a global cooling, albeit with lower estimates in the range −0.09 to −0.22°C since 1700.

[4] Forest conversion also leads to large direct emissions of CO$_2$ into the atmosphere, which, as a greenhouse gas, in turn modifies the Earth's energy balance and thus climate. Such biogeochemical effects associated with historical land cover conversion have been estimated as cumulative emissions of between 56.2 and 90.8 Pg C over the period 1920–1992 [*McGuire et al.*, 2001] using four land carbon cycle models, and 156 Pg C for the whole industrial period 1850–2000, using a simple bookkeeping approach [*Houghton*, 2003]. *McGuire et al.*'s [2001] results emphasize the importance of historical land use emissions and in addition indicate how the large and opposing effects of land cover

---

[1]Now at MetOffice (JCHMR), Wallingford, UK.

conversion and CO_2 fertilization dominated the response of the land carbon cycle over the last century.

[5] Several studies using Earth system Models of Intermediate Complexity (EMICs) have analyzed both individually and combined the biogeochemical and biogeophysical effects of historical land cover changes [*Brovkin et al.*, 2004; *Matthews et al.*, 2004]. In the work of *Brovkin et al.* [2004], biogeophysical mechanisms due to land cover change over the last millennium tend to decrease global air temperature by 0.26°C, while biogeochemical mechanisms lead to a warming of 0.18°C. The net effect is small but more pronounced over temperate and high northern latitudes where cooling due to increasing surface albedo offsets warming due to land cover change induced CO_2 emissions and other anthropogenic factors. Although *Matthews et al.* [2004] also find a small net effect, they estimate a net increase in global temperature of 0.15°C since 1700, with the biogeochemical warming exceeding the biogeophysical cooling effect. Unfortunately, an evaluation of these results remains equivocal, since the net effects are too small to discern from natural climate variability.

[6] Recent attention has focused on the influence of the land carbon cycle on future climate and atmospheric composition and the possibility of large future climate-carbon cycle feedbacks [*Cox et al.*, 2000; *Friedlingstein et al.*, 2001; *Dufresne et al.*, 2002]. These studies include land use change only in terms of global emissions used as model input. Also, *Jones et al.* [2003a] highlight the effect of current large uncertainties in land-use fluxes [*Schimel et al.*, 1996] on future atmospheric CO_2 content and climate. These models do not account for geographically explicit changes in land surface characteristics and CO_2 emissions associated with land cover changes interactive in the climate-carbon cycle model. Indeed, tropical forests shifting from carbon sink to source in high-emission scenarios ignore the fact that most of these forests may already have been deforested (see, for example, the A2 scenario in section 2).

[7] Reforestation has been proposed to help mitigate climate change. However, using the Hadley Centre General Circulation Model (GCM), *Betts* [2000] shows how reforestation in the temperate and boreal zones can also lead to a net warming, with the biogeophysical (snow-albedo feedback) exceeding biogeochemical effects, thereby accelerating rather than mitigating climate change. These findings are in line with those of *Brovkin et al.* [1999] and *Claussen et al.* [2001] on the effects of mid-high latitude deforestation. In contrast, large-scale tropical deforestation leads to net warming as the biogeochemical effect associated with increases in atmospheric CO_2 concentrations is larger than the biogeophysical effects [*Claussen et al.*, 2001]. The rate of future tropical conversion is highly uncertain, and differences between low and high scenarios relate to a range of cumulative emissions of between 47 and 132 PgC by 2100 [*Cramer et al.*, 2004]. Using a set of simplifying assumptions, *House et al.* [2002] estimate complete global deforestation to increase atmospheric CO_2 concentrations by 130–290 ppm, and complete reforestation to a reduction in future CO_2 concentrations of between 40 and 70 ppm by 2100. A more realistic land cover change scenario leads to a modest 15–30 ppm reduction by 2100. *Wigley et al.* [1997] assumed a range of 0.4–1.8 PgC/yr for the land-use source during the 1980s, which gives rise to CO_2 concentrations of between 667 and 766 ppm by 2100. However, these studies generally employ extreme scenarios of deforestation and/or reforestation with the aim to illustrate climate-vegetation interactions and do not attempt to quantify the future atmospheric CO_2 concentrations and climate based on data sets of future land cover change.

[8] *Joos et al.* [2001] applied the Bern-carbon cycle model, which includes LPJ for the land biosphere and an impulse response-empirical orthogonal function substitute of the ECHAM3/LSG AOGCM. Here six Special Report on Emissions Scenarios (SRES) emission scenarios were applied, each assuming different future economic and societal development and found atmospheric CO_2 concentration levels of between 540 and 960 ppm by 2100. *Joos et al.* [2001] postulate that land carbon storage is overestimated since no correction is made for the increasing area in cultivation, which has faster turnover times and thus reduced sink capacity than natural vegetation. Indeed, *Gitz and Ciais* [2003] estimate higher atmospheric CO_2 concentrations of 20–70 ppm by 2100 when accounting for this "Land Use Amplifier" effect, which is comparable to the climate-carbon cycle feedbacks in the IPSL GCM model [*Friedlingstein et al.*, 2001; *Dufresne et al.*, 2002], although much smaller than those in the Hadley GCM [*Cox et al.*, 2000].

[9] Only a few studies combine the effects of fossil fuel CO_2 emissions and realistic geographically explicit fields of land cover changes. *DeFries et al.* [2002] ran the CSU GCM with a future land cover data set for year 2050 from IMAGE2.1 and sea surface temperatures (SST) prescribed from present-day observations to investigate the effect of future land cover on climate. Here direct emissions from land conversion were not considered, but rather the interaction of new land cover classes with climate. Given that future land cover changes are mainly in the tropics, they found changes in plant physiology to dominate over albedo effects. Model results show that in the tropics, reduced plant productivity leads to a reduction in ratio of latent to sensible heat flux, inducing surface warming (up to 2°C) and drying. CLIMBER-2 simulations with tropical deforestation show surface warming in the case of prescribed ocean SSTs, but reveal a global-scale cooling with interactive ocean SSTs and sea ice [*Ganopolski et al.*, 2001]. The latter is explained by reduced atmospheric water vapor concentration, one of the most important greenhouse gases. *Leemans et al.* [2002] used the integrated assessment model IMAGE 2.2 to evaluate SRES narratives on future climate and atmospheric CO_2 concentration with a consistent description of land use change. By 2100, they found CO_2 concentrations for the suite of SRES narratives to range between 515 and 895 ppm. *Leemans et al.* [2002] are the first to model the consequences of the SRES emission scenarios on the carbon cycle, combined with dynamically modeled land cover change maps. However, in the work of *Leemans et al.* [2002] the biogeophysical effects of land-use change are not taken into account, given the simple climate model within IMAGE2.2. Thus far, however, more complex climate models have only
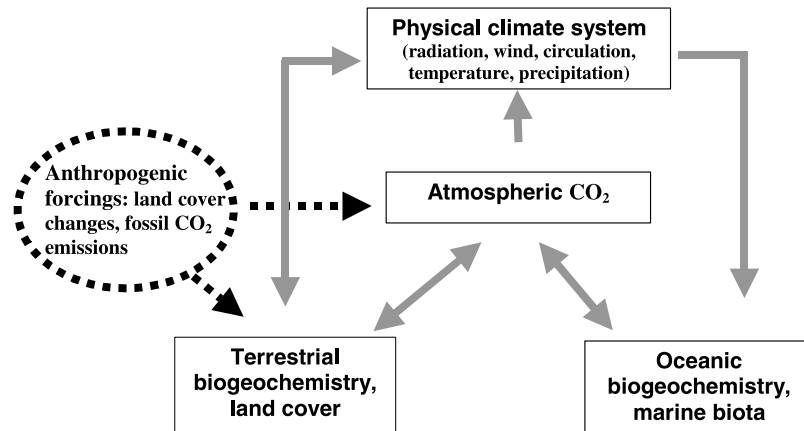
Figure 1. CLIMBER2-LPJ model design.

been run using the SRES emission scenarios, and do not consider time-varying, geographically explicit maps of land cover change, and often only use static natural vegetation.

[10] Here we present a new study which combines a consistent set of fossil fuel CO_2 emission scenarios and geographically explicit land cover change maps used to drive CLIMBER2-LPJ, a climate-carbon cycle model including dynamic vegetation and biogeophysics. Although *Leemans et al.* [2002] were the first to consistently account for both land-use and fossil fuel emissions, this study moves a step further and estimates the individual role of land use in future atmospheric CO_2 concentration (not in terms of CO_2 emissions) and temperature. In this paper we address the following questions: What is the range of future atmospheric CO_2 concentrations, and how does this compare with previously reported estimates? What are the individual contributions of fossil fuel CO_2 emissions and land cover changes for future CO_2 concentrations, and how does a reduced land sink capacity effect future atmospheric CO_2? What is the contribution of land cover changes to future global temperature rise? What is the impact of realistic, time-varying, geographically explicit fields of future land cover change on climate, and which mechanism, biogeochemical or biogeophysical, is more important and where? Alongside applying SRES future land-use scenarios in CLIMBER2-LPJ, experiments allowing complete future deforestation/reforestation are also conducted for illustration to determine the maximum uncertainty range in the effect of future land cover changes on atmospheric CO_2. The experimental design, the climate-carbon cycle model, emission scenarios, and derived land cover data sets are described in the following section. The results are then compared with literature sources and relevance of our findings discussed and conclusions drawn.

2. Methods

2.1. Model

2.1.1. Climate Component

[11] CLIMBER-2 [*Petoukhov et al.*, 2000] comprises a 2.5-dimensional dynamical-statistical atmosphere model with a coarse spatial resolution of 10° latitude and

51° longitude, a three-basin, zonally averaged ocean model, a sea-ice model with latitudinal resolution 2.5°, a terrestrial vegetation model, and the recent inclusion of ocean biogeochemistry [*Brovkin et al.*, 2002]. CLIMBER-2 is able to reproduce present-day and paleo climates [*Claussen et al.*, 1999], and compares well with more comprehensive climate models [*Ganopolski et al.*, 2001].

2.1.2. Land Carbon Cycle Component

[12] The LPJ dynamic global vegetation model [*Sitch et al.*, 2003] simulates the seasonal to century scale dynamics of land biogeochemistry and vegetation dynamics. LPJ incorporates a coupled photosynthesis–water balance scheme, plant resource competition, population dynamics, fire disturbance, and soil biogeochemistry. Compared with VECODE [*Brovkin et al.*, 1997], the existing carbon and vegetation dynamics model in CLIMBER-2, LPJ includes more plant and ecosystem mechanisms, distinguishes a larger set of 10 plant functional types (PFTs), is applied at higher spatial resolutions, typically at a 0.5° spatial resolution, and can simulate seasonal carbon and water fluxes.
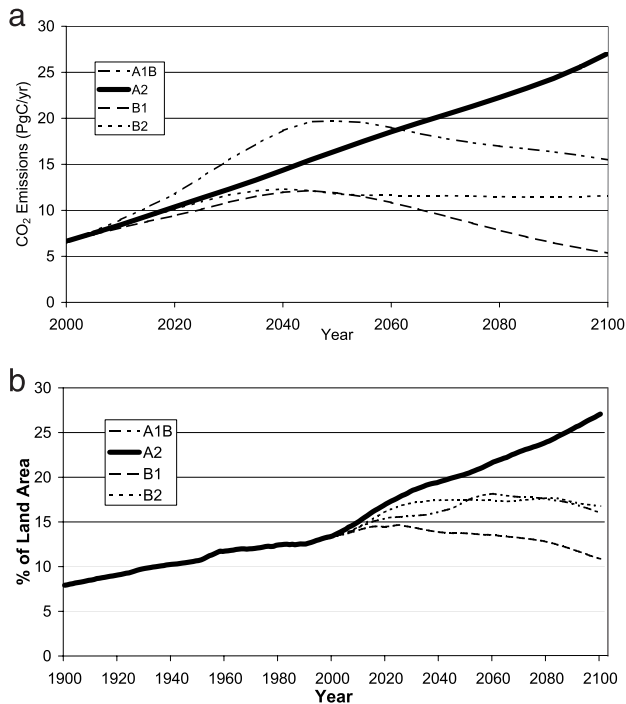
2.1.3. CLIMBER2-LPJ

[13] The CLIMBER-2 climate system model, primarily designed for century to millennial timescale applications, has been coupled with the LPJ, a higher spatial resolution vegetation–carbon cycle model suitable for seasonal-century applications. The coupled model is appropriate for decadal to century climate–carbon cycle studies. Model design is illustrated in Figure 1.

[14] Atmospheric CO_2 interacts with the ocean and vegetation components and is resolved on an annual time step,

$$C_A(t+1) = C_A(t) + \beta(E(t) + F_{OA}(t) + F_{LA}(t)). \qquad (1)$$

C_A is atmospheric CO_2 concentration (ppmv), E is fossil fuel emission (PgC/yr), F_{OA} and F_{LA} are annual ocean-atmosphere and land-atmosphere carbon fluxes (PgC/yr), respectively, and β is a conversion factor.

[15] In our coupled simulations, LPJ is run on a 0.5° spatial resolution and is called at the end of every CLIMBER-2 simulation year. CLIMBER-2 provides LPJ with monthly anomalies of surface air temperature, precipitation, and cloudiness, computed in CLIMBER-2 as a difference

Figure 2. Input data for CLIMBER2-LPJ. Temporal fields of (a) IMAGE 2.2 SRES fossil fuel CO_2 emissions 2000–2100 and (b) global total land area in cultivation for the four SRES scenarios, 1900–2100.

between current year of transient run and equilibrium pre-industrial climate state, which are added to the background climate patterns from the CRU climate data set [*New et al.*, 1999, 2000]. Absolute anomalies are used for temperature and cloudiness and relative anomalies for precipitation.

[16] Monthly land-atmosphere carbon fluxes simulated by LPJ are summed over the year and over every grid cell. This annual global sum, $F_{LA}(t)$, is passed onto CLIMBER-2 and used to calculate atmospheric CO_2 concentration and climate for the next year; see equation (1). The simulated atmospheric CO_2 is used as input for LPJ in calculating $F_{LA}(t)$ in this next year, thus creating a biogeochemical feedback between LPJ and CLIMBER-2. Biogeophysical effects of land cover changes on climate, via changes in albedo, transpiration, and roughness, are simulated by the land surface module of CLIMBER-2 accounting for changes in vegetation cover calculated by VECODE. In effect, LPJ and VECODE run in parallel, using the same SRES land cover scenarios, albeit at different spatial resolution. The former is run at finer resolution and used to infer land biogeochemistry, whereas the latter, embedded into CLIMBER-2, runs on the coarse climate model grid and used to explore biogeophysics.

2.2. Data

[17] The set of six SRES narratives on future societal and economic development has been implemented in the integrated assessment model IMAGE2.2 [*Image-team*, 2001; *Leemans et al.*, 2002], to derive a consistent description of

global environmental change, including temporally varying fields of geographically explicit land cover change and fossil fuel emissions. Scenarios based on SRES narratives A1B, A2, B1, and B2 are used here. The four SRES narratives are summarized below, with a more detailed description given by *Nakićenović et al.* [2000] and *Morita et al.* [2001].

[18] The scenario narratives are differentiated along two axes, indicated by the scenario names. Letters A and B differentiate futures emphasizing "material consumption" and "sustainability and equity," respectively, and 1 and 2 future "globalization" and "regionalization" [*Leemans et al.*, 2002]. A1B represents a future world with rapid economic growth and high technological advance, with reliance on both fossil and nonfossil energy sources. Global population peaks mid-twenty-first century and declines thereafter. This narrative assumes strong globalization, and reduced differences in per capita income between different regions. A2 describes a future fragmented and heterogeneous world, with regional emphasis on economic and social development, and a continuous increase in global population. Narrative B1 presents a convergent world emphasizing global solutions to societal, economic, and environmental issues, including the introduction of "clean" technologies. Population growth is the same as in A1B. B2 has a local emphasis, with intermediate economic development and a population that stabilizes at the end of the twenty-first century. No likelihood has been assigned to any of these scenarios.

[19] In IMAGE 2.2 the storylines of the Intergovernmental Panel on Climate Change (IPCC) scenarios have been translated into consistent assumptions for energy production and consumption, food consumption and production, and associated emissions. The energy scenarios were implemented using IMAGE's energy model TIMER. For land use, IMAGE 2.2 calculates land use and land cover on a 0.5×0.5 grid using an adapted version of the AEZ model and a set of simple allocation rules. In total, 17 biome types and 5 land use types are distinguished. In this study, only land use type agricultural land is considered, which includes croplands, land for modern biofuels, and pastures. The other time variant land use types for the SRES scenarios are forest regrowth resulting from either forestry or agricultural land abandonment. The former is not considered in this study whereas the latter is explicitly modeled by CLIMBER2-LPJ.

[20] Historical changes in cropland area on a $0.5°$ grid are taken from *Ramankutty and Foley* [1999] for the years 1700–1990. The IMAGE SRES scenarios of future land cover changes supplement these historical data for years 1990 through 2100, using an anomaly approach with reference year 1990. After 1990, for each grid cell, changes to/from agricultural land in the IMAGE scenarios are used to update the *Ramankutty and Foley* [1999] historical map of 1990. For grid cells where there is disagreement between the two land cover data sets in 1990, in terms of whether a grid cell is agricultural land or not, the first land cover changes after 1990 are not considered.

[21] Future fossil fuel CO_2 emissions derived from the four SRES narratives as implemented by IMAGE are added to the historical time series of CO_2 emissions from
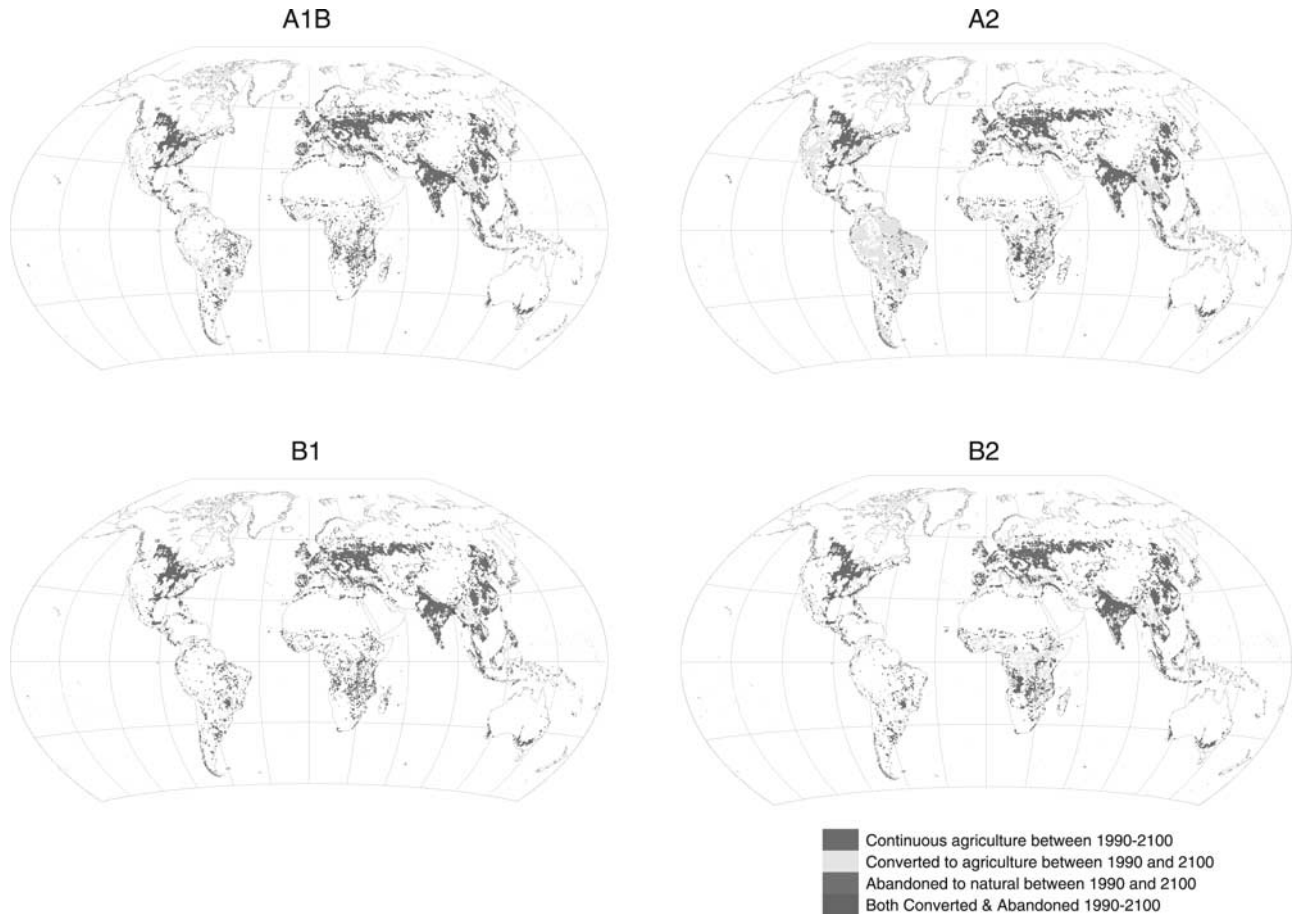
Figure 3. Geographically explicit IMAGE 2.2 land cover changes, 1990–2100, for four SRES scenarios; anomaly approach to RF historical cropland data set. See color version of this figure at back of this issue.

G. T. Marland et al. (Global, regional and national fossil fuel CO_2 emissions, from Trends database, Carbon Dioxide Information Analysis Center, Oak Ridge National Laboratory, Oak Ridge, Tennessee, 2002, available at http://cdiac. esd.ornl. gov/trends.emis.meth_reg.htm). Non-CO_2 greenhouse gases and future aerosol emissions were not accounted for in CLIMBER2-LPJ. Figure 2 shows the global total land area in agriculture for the four SRES scenarios, 1900–2100, and IMAGE SRES fossil fuel CO_2 emissions 2000–2100.

[22] A2 and B1 represent the extremes in terms of both future fossil fuel CO_2 emissions and land cover changes relative to the present day, with A2 (having the highest emissions and largest deforestation) the worst-case and B1 (with the lowest emissions and a net reforestation) the most benign scenario. For scenarios A1B and B1, the temporal development of fossil fuel CO_2 emissions follow trends in global population and a compounded effect of income growth per capita and technological improvement, increasing from 6.3 PgC/yr in 1995, peaking at 19.7 and 12.2 PgC/yr, respectively, around 2050 and declining thereafter. By 2100, emissions fall to 15.5 PgC/yr for A1B, and at 5.4 PgC/yr fall below present-day emissions for scenario B1. The differences are mainly caused by a more energy-intensive style of

consumption assumed in A1B. B2 fossil fuel CO_2 emissions also increase at a rate similar to B1 from 1995, peaking in 2040 at 12.3 PgC/yr, and remain approximately unchanged thereafter (driven by a stabilizing population). A2 emissions increase continuously over the whole period, albeit at an initial rate between those of A1B and B1 as a result of development in low-income countries. A2 emissions, however, surpass A1B by 2060, reaching 27 PgC/yr in 2100. The main cause of this is the strong reliance on coal in many developing regions.

[23] In 1990, 12.5% of the global land area is in cropland. Future scenarios diverge with an additional 14.5% of the global land area in agriculture by 2100 in A2, and −1.7%, representing net land abandonment, in B1. The main drivers of future agricultural land area are increase in food consumption, dietary shifts, and increases in yields. In B1 a stabilizing population, relatively fast yield increases, and low-meat consumption result in a net decrease in agricultural land over the whole century (but with a peak in 2010). Reforestation mainly occurs in temperate zones of the Former Soviet Union, because of future increases in agricultural productivity and a declining population. A1B and B2 show similar temporal developments, but here increased food demand offsets technological progress, resulting in a moderate addi-

Table 1a. Baseline CLIMBER2-LPJ Simulations

Acronym	IMAGE 2.2 SRES Fossil Fuel Scenario, Years 2000–2100	Scenario of Land Cover Changes, 1990–2100
A1B	A1B	A1B, IMAGE 2.2
A1B_nol	A1B	no changes in agricultural land after 1990
A2	A2	A2, IMAGE 2.2
A2_nol	A2	no changes in agricultural land after 1990
B1	B1	B1, IMAGE 2.2
B1_nol	B1	no changes in agricultural land after 1990
B2	B2	B2, IMAGE 2.2
B2_nol	B2	no changes in agricultural land after 1990

tion of 3.5% and 4.2%, respectively, of agricultural lands by 2100. A regional breakdown (Figure 3) shows for all scenarios large-scale land conversions in Africa and Southeast Asia, and in particular for scenarios A2 and B2 (the narratives stressing future "regionalization").

[24] A2 predicts extensive land conversions in all tropical and subtropical regions, and in North America. In fact, most land suitable for agriculture, i.e., all areas except deserts, boreal forests, tundra, and mountain regions, are in land use by 2100 in A2. This extreme land use is needed to feed the 15 billion people by the end of the twenty-first century who have high-caloric dietary demands in combination with low agro-technological developments. Only a small amount of area in Europe is abandoned to natural vegetation. Although the temporal dynamics of total land in agriculture are similar between A1B and B2, regional differences are apparent. Aside from large-scale land conversion in Africa and Southeast Asia, B2 projects some land conversion in other tropical and subtropical regions and significant land abandonment in east Europe. In contrast, A1B projects land conversion in eastern North America, greater conversion in South America than B1 and B2 (because South America becomes an important exporting region in the globalized A1B world), and land abandonment in China (because of fast technological developments). B1 represents the most benign scenario with land conversion in Southeast Asia (except China), and both conversion and subsequent abandonment between 1990 and 2100 in Africa. In China, East Europe, and the former Soviet Union, large areas of agricultural lands are abandoned by 2100.

2.3. Experimental Design

[25] As LPJ simulates fire disturbance, it needs year-to-year variability in climate in order to correctly simulate global vegetation. CLIMBER-2 simulates the long-term (decadal to millennia) trend in climate, but not interannual climate variability. To account for the latter in the coupled simulations, we used a cyclic replication of CRU monthly climatology for years 1901–1930 during the 1000-year spin-up. These 30 years are less affected by anthropogenic climate change than subsequent years, and therefore the corresponding climatology is closest to the prehistorical climate. The LPJ model is initialized with land cover for the year 1901 after running for a spin-up using pre-1900 atmospheric CO_2 and climate patterns simulated by CLIMBER-2. Reconstructed changes in insolation and volcanic aerosols are used during model spin-up. Details of applied natural forcings accounted for are described by *Brovkin et al.* [2004].

[26] For each transient year (1901–2100), a year between 1901 and 1930 was randomly selected. The corresponding set of 12 months CRU climatology are updated with climate anomalies from CLIMBER-2 and used to drive LPJ. We repeated coupled simulations 20 times, with a different random sequence of years of CRU climatology, and calculate mean average and standard deviation of the simulation ensemble. The combined R&F/IMAGE 2.2 land cover change data set (described above) was used as the land cover forcing after the year 1901. Land carbon fluxes were calculated in accordance with the approach of *McGuire et al.* [2001].

[27] The suite of experiments using CLIMBER2-LPJ is summarized in Tables 1a and 1b. Baseline simulations (Table 1a) A1B, A2, B1, and B2, use both the respective scenarios of IMAGE 2.2 SRES fossil fuel CO_2 emissions (2000–2100) (SO_2 and non-CO_2 greenhouse gases are not included) and land cover changes 1990–2100 to drive CLIMBER2-LPJ. To infer the individual contributions of future fossil fuel emissions and land cover changes to future atmospheric CO_2 and climate, a no land cover change simulation (_nol) was conducted for each IMAGE 2.2 SRES scenario using the fossil fuel CO_2 emissions only, with no change in cropland area after 1990.

[28] To portion the net climate response into individual, geographically explicit biogeophysical and biogeochemical contributions, two further experiments were conducted for scenarios A2 and B1 (Table 1b). In A2phys, only the

Table 1b. CLIMBER2-LPJ Supplementary Simulations With A2 and B1 SRES Scenarios

Acronym	IMAGE 2.2 SRES Fossil Fuel Scenario, Years 2000–2100	Scenario of Land Cover Changes, 2000–2100	Biogeophysical Effect of Land Cover Changes	Biogeochemical Effect of Land Cover Changes
		Sensitivity Analysis		
A2max	A2	complete deforestation by year 2100	yes	yes
A2min	A2	complete reforestation by year 2100	yes	yes
B1max	B1	complete deforestation by year 2100	yes	yes
B1min	B1	complete reforestation by year 2100	yes	yes
		Mechanism Analysis		
A2phys	A2	A2, IMAGE 2.2	yes	no
A2chem	A2	A2, IMAGE 2.2	no	yes
B1phys	B1	B1, IMAGE 2.2	yes	no
B1chem	B1	B1, IMAGE 2.2	no	yes

Table 2. CLIMBER2-LPJ Simulation Results

	Atmospheric CO_2 Content 2100, ppm	Cumulative Land Uptake, 2000–2100, PgC	Temperature Change, 2000–2100, °C
	Baseline Simulations		
A1B	847	190	2.6
A1B_nol	789	328	2.4
A2	957	9	2.7
A2_nol	830	312	2.4
B1	592	212	1.7
B1_nol	572	260	1.5
B2	677	156	2.1
B2_nol	631	272	1.8
	Sensitivity Analysis		
A2max	1288	−787	3.1
A2min	806	382	2.5
B1max	980	−760	2.4
B1min	552	321	1.6

biogeophysical effect of future land cover changes on future climate and atmospheric CO_2 is considered. Here CLIMBER-2 is driven with both the IMAGE 2.2 SRES fossil fuel and land cover changes scenarios; that is, land surface characteristics such as albedo and surface roughness are modified according to future land cover changes. LPJ is run with no change in agricultural land area after 1990. Hence the biogeochemical fluxes supplied by LPJ to CLIMBER-2 at the end of each year do not include fluxes associated with future changes in agricultural land area. In A2chem, only the biogeochemical effect of future land cover changes is considered. CLIMBER-2 is driven with the IMAGE 2.2 fossil fuel CO_2 emission scenario only, with fixed agricultural land areas from 1990 onward. Nevertheless the annual fluxes supplied by LPJ include the effects of future changes in agricultural land extent.

[29] In order to quantify the "Land Use Amplifier," the impact of reduced natural land cover, and hence land

storage capacity, on future atmospheric CO_2 content, two additional simulations (A2fix and A2amp) were conducted. In A2fix, the CO_2 concentrations and climate anomalies from baseline A2 are used to drive LPJ with fixed land cover changes after 1990 and annual global land fluxes from LPJ are recorded. The difference in land fluxes between baseline A2 and A2fix, $\Delta F_{LA}(t)$, integrated over the whole simulation period represents the effect of reduced natural land cover on the capacity of the land biosphere to store carbon, added to the land use flux, expressed in terms of cumulative emissions. Simulation A2amp repeats the A2_nol simulation adding the $\Delta F_{LA}(t)$ to the fossil fuel CO_2 emission. The difference between atmospheric CO_2 concentrations in A2 and A2amp gives an estimate of the "Land Use Amplifier."

[30] Additional sensitivity studies using CLIMBER2-LPJ are described in Table 1b. Scenarios A2 and B1 were selected for the sensitivity study as they represent the worst and most benign cases, respectively. A2max represents a simulation with complete "deforestation" by 2100. CLIMBER2-LPJ is run as in baseline A2 until year 2000. In each subsequent year, 1% of the remaining 0.5° grid cells not in land use are randomly selected and converted to agriculture. Again following the approach of *McGuire et al.* [2001], actual crop production is governed by individual grid cell climatology and soils. The A2 fossil fuel CO_2 emission scenario is used throughout. Similarly for A2min, in each year after 2000, 1% of the agricultural grid cells are abandoned to natural vegetation. A2min represents a scenario with complete "reforestation" by 2100 (i.e., returning to the natural vegetation, and allowing for vegetation changes associated with the climatic change).

[31] There are certain limitations in the experimental design related to the model capabilities. For instance, LPJ does not simulate emissions of CH_4 and N_2O associated with land cover. Also, the current version of CLIMBER-2
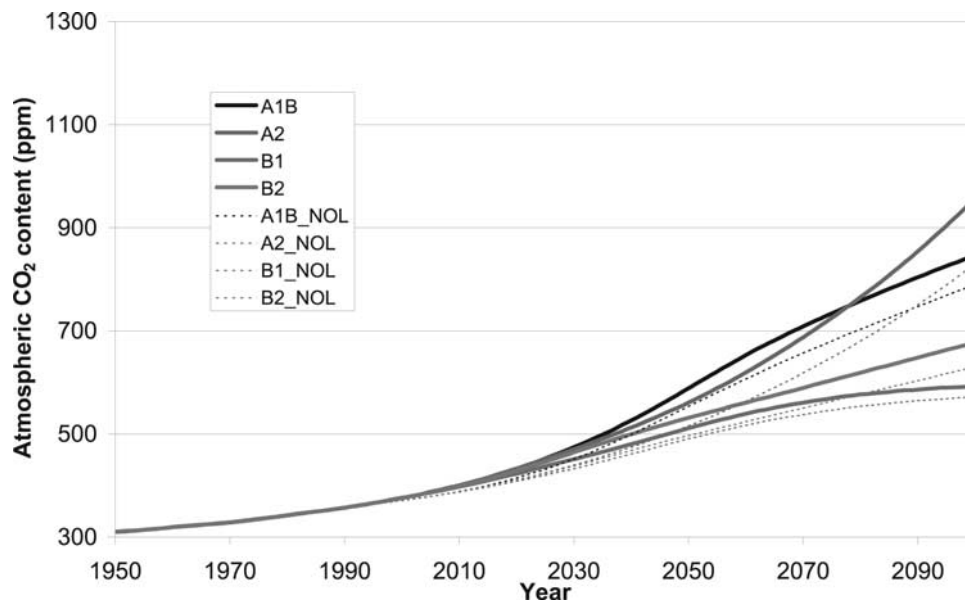
Figure 4. Atmospheric CO_2 concentrations 1950–2100 for four SRES scenarios, and simulations with no land cover changes after 2000. See color version of this figure at back of this issue.
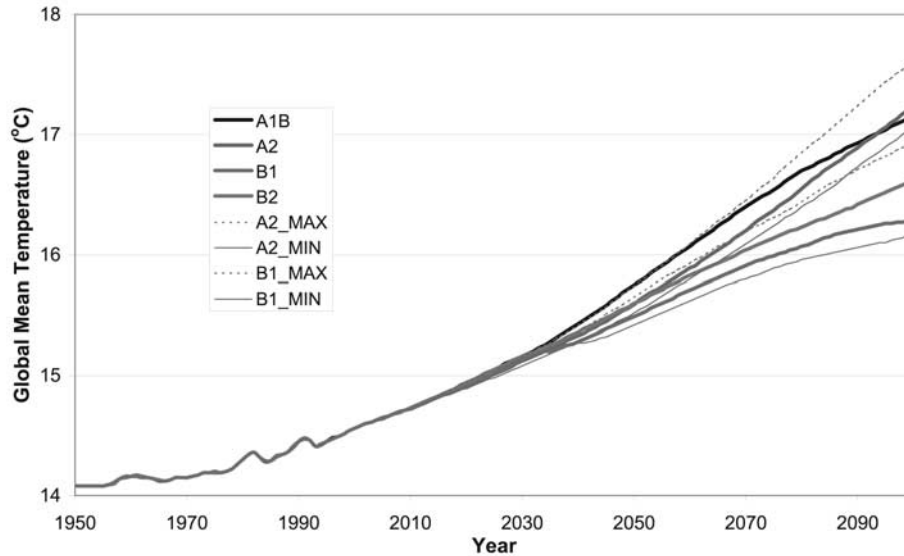
Figure 5. Global mean annual temperature for the four SRES scenarios. See color version of this figure at back of this issue.

does not account for the radiative effects of non-CO_2 greenhouse gases (e.g., CH_4, N_2O) and sulfate aerosols. Therefore, in all simulations, we neglected climatic effects of the non-CO_2 greenhouse gases and aerosols. This may lead to an underestimation of climate change in the future (see section 4). However, the effect of this limitation on the difference between two, with and without land-use simulations, for example, A2-A2_nol, is likely to be of secondary order, since forcings are unaccounted for in both simulations. Hence these results on the impact of land cover changes on atmospheric CO_2 and climate should be relatively robust.

3. Results

[32] Results from all simulations for future atmospheric CO_2 content, and global temperature change relative to the present day, are presented in Table 2.

3.1. Impact of SRES Scenarios on Future Atmospheric CO_2

[33] In 2100, atmospheric CO_2 ranges from 592 ppm (B1) to 957 ppm (A2) (Figure 4). By 2100, atmospheric CO_2 has stabilized at 592 ppm for B1. In A1B, atmospheric CO_2 is still increasing by 2100 but atmospheric CO_2 is only slowly approaching its asymptote, even though land cover is stable and annual emissions are decreasing throughout the latter half of the twenty-first century. With an almost linear increase in land conversion and fossil fuel CO_2 emissions, atmospheric CO_2 content in A2 is ever increasing during the latter half of the twenty-first century, implicating positive feedbacks in the climate-carbon system.

[34] Differences in atmospheric CO_2 concentration between A2 and A2_nol represent the net effect of land cover changes of SRES scenario A2 on atmospheric composition (likewise for A1B, B1, B2). It primarily includes the

land-use conversion flux, but also secondary biogeochemical effects like CO_2 fertilization in deforested land, the "land-use amplifier," and the synergy between the biogeophysical and biogeochemical effects of land cover changes.

[35] The absolute difference between the A2 and A2_nol is increasing throughout the simulation period. In the first order this is explained by ongoing deforestation, decomposition of product pools, and excess soil organic matter associated with past conversion, with additional effects of the "land use amplifier" and CO_2 fertilization mechanism.

[36] The "Land Use Amplifier," given as the difference in atmospheric CO_2 content between simulations A2 and A2amp represents a very small 4 ppm, compared to 46 ppm for SRES A2 from *Gitz and Ciais* [2003]. Note results from the present study are not strictly comparable because dynamic vegetation in CLIMBER2-LPJ leads to changes in vegetation cover and biomass. Also, biogeophysical cooling induces a relative reduction in heterotrophic respiration.

[37] The maximum contribution of land cover changes to future atmospheric CO_2 among the four SRES scenarios represents a modest 127 ppm (A2-A2_nol). In contrast, the minimum contribution represents only 20 ppm for SRES B1. In relative terms, land cover changes contribute between 9 and 22% (B1 and A2, respectively) to future atmospheric CO_2, with the remainder attributable to fossil fuel CO_2 emissions.

3.2. Effects of Future Land Cover Changes on Climate

[38] Global mean annual temperatures for the four SRES scenarios are shown in Figure 5. By 2100, increases in future temperatures, relative to year 2000, range between 1.7°C (B1) and 2.7°C (A2). This relatively small warming can be explained by neglecting the radiative effects of non-CO_2 greenhouses gases and sulfate aerosols in the experiments. While at present both effects almost compensate each other,
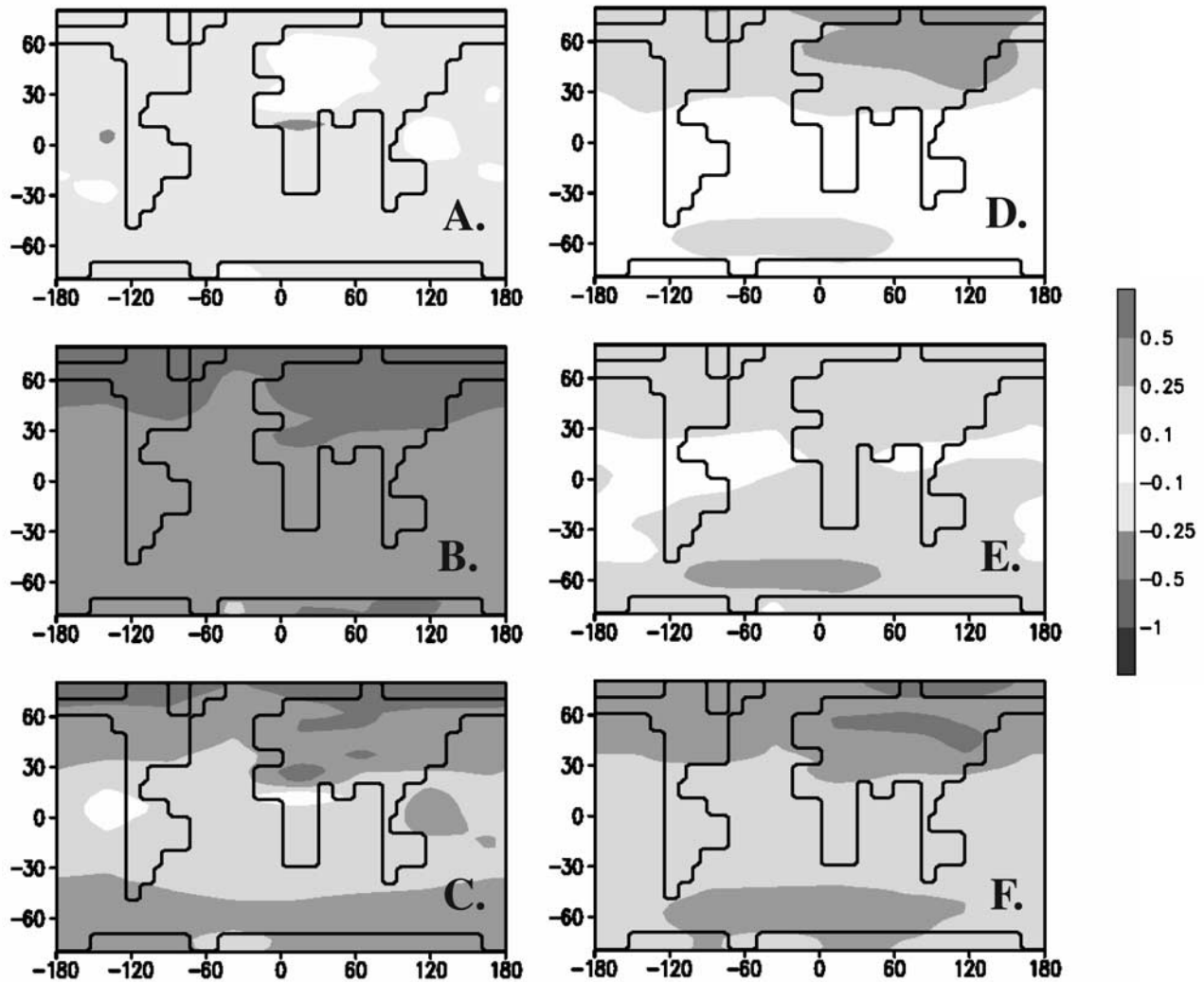
Figure 6. Simulated changes in mean annual temperature (°C) due to land cover changes only. (a) A2 biogeophysical effect (A2phys-A2_nol), (b) A2 biogeochemical effect (A2chem-A2_nol), (c) A2 net effect (A2-A2_nol), (d) B1 biogeophysical effect (B1phys-B1_nol), (e) B1 biogeochemical effect (B1chem-B1_nol), and (f) B1 net effect (B1-B1_nol). See color version of this figure at back of this issue.

in the SRES narratives the warming effect of CH_4, N_2O, and other non-CO_2 greenhouse gases increases in time, while the cooling effect of SO_2 hardly increases or even declines [*IMAGE-team*, 2001; *Cubasch et al.*, 2001]. Temperature changes for A1B and A2 are similar by 2100, despite a large CO_2 difference of 110 ppm between scenarios. This is mostly explained by biogeophysical cooling due to the stronger deforestation in the A2 scenario (see also Figure 7 in section 3.3). In addition, the difference in timing of CO_2 emissions results in higher CO_2 concentrations in the 2050s and consequently earlier warming for A1B compared with A2.

[39] In order to attribute these increases in global temperature to the individual, regionally varying contributions of biogeophysics and biogeochemistry, additional simulations A2phys, B1phys and A2chem, B1chem were conducted. A2 and B1 represent the extreme scenarios in terms of total area

in cultivation by 2100 and have markedly different regional land cover dynamics, with large-scale tropical deforestation and temperate reforestation in A2 and B1, respectively.

[40] Global maps of the biogeophysical (e.g., A2phys-A2_nol), biogeochemical (e.g., A2chem-A2_nol), and combined (e.g., A2-A2_nol) effects of land cover changes on future temperature between 1990 and 2100 are shown for scenario A2 and B1 in Figure 6.

[41] In A2 the biogeophysical effect leads to a cooling of between 0.0°C and −0.5°C in all regions. Although the largest changes in land cover are projected for the tropics and subtropics, deforestation in these regions can also lead to a cooling in higher latitudes. Here reduced transpiration in tropical ecosystems leads to a weaker hydrological cycle and thus less water vapor, a strong greenhouse gas, in the atmosphere. Temperatures are further reduced in high lat-
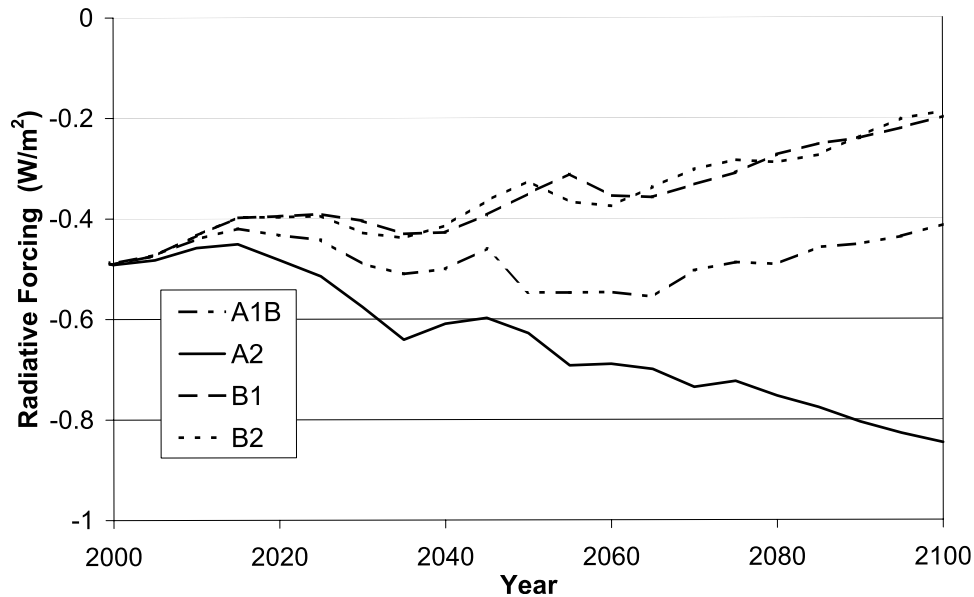
Figure 7. Globally averaged radiative forcing at the top of atmosphere due to land cover changes in land cover (in W/m^2) for the four SRES scenarios. Radiative forcing only accounts for the shortwave solar radiation and is due to changes in land surface albedo. Radiative forcing is computed relative to prehistoric (1000 A.D.) distribution of vegetation, which was close to potential natural vegetation.

itudes via the sea ice-albedo feedback [*Ganopolski et al.*, 2001]. Given a net increase in agricultural land, in all SRES scenarios the biogeochemical effect is expected to be a climate warming. A2 represents the most extreme scenario of land conversion, and hence projected warming is the most pronounced with regional temperature increases typically between 0.25°C and 0.5°C, and above in high latitudes. In the combined A2 simulation, biogeochemical warming due to CO_2 emissions mainly associated with future tropical and subtropical land conversion is larger over all land regions than the biogeophysical cooling induced by corresponding changes in surface energy and moisture fluxes. Nevertheless, despite large-scale land cover changes in the tropics and subtropics, which cause local temperature increases of 0°–0.25°C, impacts are strongest at higher latitudes with temperature increases above 0.25°C.

[42] In B1, biogeochemical warming is smaller than in A2 with regional temperature increases between 0°C and 0.25°C. This is not surprising given that scenario B1 projects the lowest levels of tropical and subtropical land conversion, and extensive land abandonment in the former Soviet Union. In B1 the biogeophysical effect leads to a warming, with annual temperature increases of between 0.1° and 0.25°C over North America, southern Europe, and South Asia, and increases between 0.25°C and 0.5°C over most of Eurasia. The combined biogeochemical and biogeophysical effect for B1 leads to temperature increases of 0.1°–0.25°C over low latitudes, between 0.25°C and 0.5°C for latitudes above 30°, and above 0.5°C across a band over Eurasia.

[43] In A2 and B1 the combined effect of land-use change (physical and chemical) results in similar global and local temperature changes (see also Table 2). However, the two feedbacks contribute differently per scenario. In B1, the

biogeophysical effect is a warming, because of temperate forest regrowth. The biogeochemical effect is very small, and therefore the combined effect is comparable with the results from A2. In A2, biogeochemical effects are very large because of extensive land conversion, but temperature increases are reduced by the opposing cooling biogeophysical effect.

[44] However, the net effect of land cover changes on regional precipitation differs among scenarios. The biogeophysical effect of tropical deforestation in A2 is to reduce annually averaged rainfall over the Amazon and Central Africa by up to 0.5 mm/day and 0.25 mm/day, respectively (not shown). The biogeochemical effect of land cover changes is to increase average precipitation across the tropics and subtropics by up to 0.25 mm/day. The net effect is a reduction in rainfall of up to 0.25 mm/day over most of Amazonia. Although this effect is small (~90 mm/yr) relative to the high annual precipitation in the region, it is important since it will augment a possible reduction in future precipitation already predicted over this region by some climate models (e.g., HadCM3 predicts rainfall reduction of ~600 mm/yr, without accounting for the effect of geographically explicit land cover changes). However, in B1 both the biogeochemical and biogeophysical effects of future land cover changes on precipitation changes are minor. Given that the biogeochemical effect represents only an increase in atmospheric CO_2 of 20 ppm, as opposed to 127 ppm for A2, this is not surprising.

3.3. Effects of Future Land Cover Changes on Radiative Forcing

[45] Figure 7 shows the temporal dynamics of radiative forcing associated with the biogeophysical effect of land use (changes in surface albedo only) for the four SRES
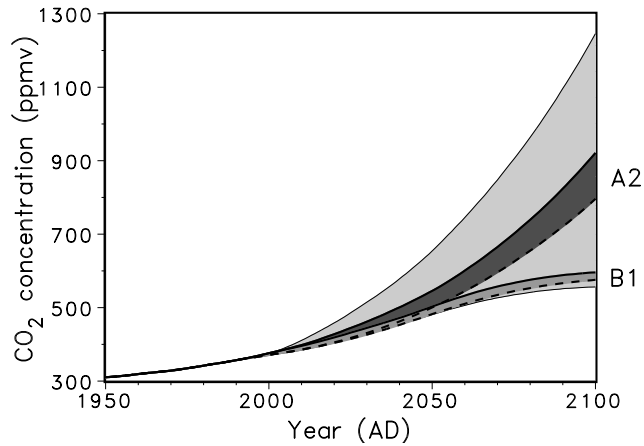
Figure 8. Atmospheric CO_2 concentrations 1900–2100 for complete deforestation, reforestation, and no future land use change for A2 and B1. The light shaded area shows the range in CO_2 concentrations between A2max and B1min. The dark and medium-dark shaded areas show CO_2 concentrations between A2/A2_nol and B1/B1_nol, respectively.

scenarios. Compared to prehistoric times (1000 AD), present-day radiative forcing of land use is about -0.5 W/m^2 (or -0.3 W/m^2 compared to the pre-industrial period, 1800 A.D.).

[46] For the scenarios B1 and B2, negative radiative forcing of land cover changes decreases in absolute value during the twenty-first century, which is primarily attributed to the land abandonment in the boreal zone, where land cover changes exert the strongest effect on radiative fluxes due to large differences in surface albedo between forest and croplands during winter. Conversely, in A2 the negative radiative forcing due to land-cover changes continues to grow in absolute value, which partly compensates the positive radiative forcing related to additional CO_2 released to the atmosphere due to land use. In absolute terms, changes in radiative forcing due to the biogeophysical effect are comparable to radiative forcing of CO_2 changes associated with additional CO_2 emission due to land use.

3.4. Impact of Future Reforestation and Deforestation on Atmospheric CO_2

[47] For emissions scenario A2 the difference in atmospheric CO_2 in year 2100 between complete future deforestation (1288 ppm) and reforestation (806 ppm) is 482 ppm, comparable to the range associated with uncertainties in fossil fuel CO_2 emissions alone. This range increases to 736 ppm when for illustration the lowest (B1) and highest (A2) fossil fuel CO_2 emission scenarios are completely reforested and deforested, respectively, by 2100 (Figure 8).

[48] For SRES scenario B1, the difference between complete deforestation (980) and reforestation (552) is 428 ppmv, a value similar to that obtained for A2. In the simulation B1max, atmospheric CO_2 is higher than in A2 baseline; that is, results for the whole set of CO_2 emission scenarios lie within the range of results for B1 simulations,

which differ only in assumptions regarding future land cover changes. Like with A2 simulations discussed above, this stresses a potential role of land cover in CO_2 change as large as that for fossil fuel CO_2 emission scenarios.

[49] Temperature changes are also influenced by deforestation/reforestation. The best example is that global temperature in 2100 is slightly higher in A2min (reforestation) than in B1max (deforestation), despite very different CO_2 levels of 806 and 980, respectively. Although CO_2 concentrations are higher by 174 ppm in B1max than in A2min, the biogeophysical cooling effect of completely deforested land is very pronounced and completely offsets the biogeochemical warming effect.
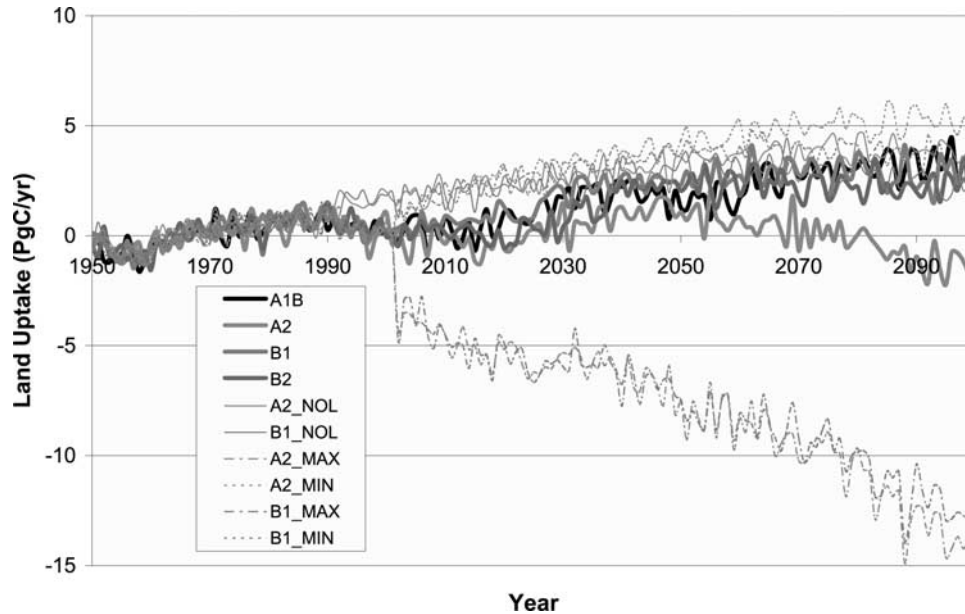
3.5. Future Land Uptake

[50] Net land uptake of atmospheric CO_2, which accounts for both carbon sequestration in natural ecosystems and emissions associated with land cover changes, varies widely among scenarios (Figure 9; Table 2). A2 is the scenario with the greatest land conversion. Initially, there is a moderate increasing trend in net land uptake of up to $1-2$ PgC/yr by 2050. After 2050 the trend is reversed, and becomes a net source after 2070, releasing between $1-2$ PgC/yr by 2100. Other SRES baseline simulations show a net uptake increasing up to 2050, saturating thereafter at $\sim 2-4$ PgC/yr. Simulations with no change in future land use, for example, A2_nol, follow a similar trend, albeit with larger annual land uptake because of lack of deforestation fluxes.

[51] Despite future land cover conversion, all baseline SRES scenarios predict future cumulative net land uptake of carbon, mainly driven by CO_2 fertilization. Cumulative net land uptake over the twenty-first century ranges from 9 PgC (A2) to 212 PgC (B1), with A1B (190 PgC) and B2 (156 PgC), close to the upper end of the range.

4. Discussion

[52] For comparison purposes, Table 3 presents the current results alongside others reported in the literature. These projections are higher than the range of 545 ppm (B1) and 846 ppm (A2) reported by *Prentice et al.* [2001], although still within their uncertainty bounds due to incomplete understanding of climate sensitivity and the carbon cycle. Using the same future fossil fuel CO_2 emissions and land cover change scenarios, *Leemans et al.* [2002] project, using IMAGE 2.2, considerably smaller future atmospheric CO_2 concentrations of between 515 ppm and 755 ppm. Since CLIMBER2-LPJ and IMAGE2.2 have similar climate sensitivity ($2.5°–2.6°C$ for CO_2 doubling), results differ mainly owing to the inclusion of the biogeophysical effect in CLIMBER2-LPJ, and differences in parameterizations of terrestrial and ocean biogeochemical processes. For example, the models differ in parameterizations of the heterotrophic respiration response to temperature. Indeed, *Jones et al.* [2003b] have shown the future source/sink behavior of the terrestrial carbon cycle to be particularly sensitive to the temperature response function of soil respiration. The models may also disagree owing to differences in initial biomass and soil carbon pools.

[53] The maximum contribution of land cover changes to future atmospheric CO_2 among the four SRES scenarios

Figure 9. Net land uptake for four SRES scenarios. See color version of this figure at back of this issue.

represents 127 ppm. Land conversion fluxes are primarily responsible. In relative terms, this represents 22% of the combined effect of future fossil fuel CO_2 emissions and changing land use on atmospheric CO_2 for A2. Among SRES scenarios the relative contribution of land cover changes ranges between 9% (B1) and 22% (A2). In equivalent experiments, *Leemans et al.* [2002] estimate a larger range between 0% (B1) and 24% (A2). Using several model and land use data set combinations, *Brovkin et al.* [2004] found a declining contribution from 36–60% to 4–35% over the historical periods 1850–1960 and 1960–2000, respectively. Over the latter period, CLIMBER2-LPJ esti-

mates an average contribution of 18%. Hence the relative role of land cover changes in atmospheric CO_2 growth is expected to decline further in the future compared with the present day. The current study confirms the overall finding of *House et al.* [2002] that fossil fuel emissions will dominate future atmospheric CO_2 concentrations, the effects of land cover change being modest in comparison.

[54] The magnitude and temporal trend in land uptake is similar to a stand-alone LPJ simulation with natural vegetation forced with HadCM2 future climate (IS92A) [*Cramer et al.*, 2001]. However, S. Schaphoff et al. (Terrestrial biosphere carbon storage under alternative climate projec-

Table 3. Comparison of CLIMBER2-LPJ With Other Studies

	This Study	Cubasch et al. [2001]	Prentice et al. [2001][a]	Joos et al. [2001]	Leemans et al. [2002][b]	Johns et al. [2003][c]	House et al. [2002]	Gitz and Ciais [2003]
			Atmospheric CO_2 Content 2100, ppm					
A1B	847		710	703	755			
A2	957		846	830	871	819		882
B1	592		545	540	515	531		500
B2	677		616	605	606	604		609
Contribution of land cover changes	20 to 127						15 to 30	
Net land use amplifier	4							20 to 70 (46[d])
Reforestation [A2min-A2_nol] (B1)	−24 (−20)						−40 to −70	
Deforestation [A2max-A2_nol] (B1)	458 (408)						130 to 290	
			Temperature Change, 2000–2100, °C					
A1B	2.6	2.8		2.3	3.0			
A2	2.7	3.6		2.9	3.3	3.1		
B1	1.7	1.8		1.6	1.9	1.9		
B2	2.1	2.5		2.0	2.5	2.2		

[a]Taken as the average from the ISAM (reference) model and Bern-CC (reference) model.
[b]Temperature change, 1995–2100, °C.
[c]Temperature change, calculated as the difference in average temperature between two periods, (2069–2099) and (1969–1999).
[d]This is the net land use amplifier for SRES scenario A2 from *Gitz and Ciais* [2003].

tions, submitted to *Climate Change*, 2005) emphasize the uncertainty in both sign and magnitude of the land uptake associated with choice of climate model. The standard experiment of *Joos et al.* [2001] has the same temperature sensitivity as CLIMBER-2 ($2.5^\circ C/2xCO_2$), and also utilizes LPJ as the land carbon cycle model. Comparing studies is especially useful to infer the effect of geographically explicit land cover changes. For A1B, *Joos et al.* [2001] project an average net land uptake of 2.3 PgC/yr during the twenty-first century (F. Joos, personal communication, 2004). These results agree quantitatively with the current study estimates for A1B of an increasing flux between 0 and 3.5 PgC/yr, with an average of 1.9 PgC/yr. In the present study, carbon sequestration is lower than in the study by *Leemans et al.* [2002], who estimate net land uptake at 3.6 PgC/yr and 5.3 PgC/yr in individual years 2050 and 2100, respectively. Indeed, the larger land uptake of *Leemans et al.* [2002] can partially explain the differences in atmospheric CO_2 levels between the two studies. *Joos et al.* [2001] and *Leemans et al.* [2002] estimate net land uptake for A1B of 232 PgC and 340 PgC, respectively, over the twenty-first century, both higher than the 190 PgC estimated here. Despite higher CO_2 concentrations of 144 ppm in 2100 compared with A1B of *Joos et al.* [2001], and with the same temperature sensitivity, the present study predicts lower global mean temperatures. Note that some biogeophysical agents (e.g., dust) and greenhouse gases (CH_4, N_2O emissions) were not considered in our simulations. The biogeographical cooling associated with land cover changes (not considered by either *Joos et al.* [2001] or *Leemans et al.* [2002]) counterbalances the biogeochemical effects, thereby modulating the otherwise large increases in temperature.

[55] Additionally, *Joos et al.* [2001] postulate the potential land carbon storage to be overestimated, since no correction is made for an increasing area in cultivation, which has faster turnover times and thus reduced sink capacity than natural vegetation. Indeed, *Gitz and Ciais* [2003] estimate this effect as an additional 20–70 ppm by 2100, with a net "Land Use Amplifier" for SRES A2 of 46 ppm. In comparison, this study estimates the net "Land Use Amplifier" as an additional 4 ppm.

[56] CLIMBER2-LPJ projects increases in future temperatures to range between $1.7^\circ C$ (B1) and $2.7^\circ C$ (A2) relative to year 2000. Model results compare well with those of *Joos et al.* [2001]. Results for B1 and B2 are the same as *Joos et al.* [2001], whereas for A2, CLIMBER2-LPJ projects lower temperatures by $0.2^\circ C$. This can be attributed to biogeophysical cooling not included by *Joos et al.* [2001], with A2 the scenario with the most extensive tropical land conversion, although some difference might be due to different climatic forcings accounted for by *Joos et al.* [2001]. Given that CLIMBER-2 has a moderate climate sensitivity ($2.5^\circ C/2xCO_2$), these estimates of future temperature should be considered conservative. Indeed, the average increase in global temperature since year 2000 for a simple climate model separately tuned to simulate the response of several complex Atmospheric-Ocean General Circulation Models (AOGCMs) ranges between $1.8^\circ C$ (B1) and $3.6^\circ C$ (A2) for the four scenarios used here [*Cubasch et*

al., 2001]. Variation in results among "AOGCM analogues" is large, with an uncertainty of above $1^\circ C$ for all four scenarios and $\sim 2^\circ C$ for A2. *Leemans et al.* [2002] project future temperature increases since 1995 of between $1.9^\circ C$ (B1) and $3.3^\circ C$ (A2) for the same CO_2 emissions and land cover change scenarios as in the present study. However, *Leemans et al.* [2002] also account for emissions of the non-CO_2 greenhouse gases and SO_2. Although at present the warming effect of the non-CO_2 greenhouse gases approximately cancels the cooling effect of aerosols, in the future the non-CO_2 greenhouse gas warming is expected to exceed, by several times, the cooling aerosol effect (emissions of non-CO_2 greenhouse gases are expected to increase and aerosol emissions to decrease) [*Cubasch et al.*, 2001; *IMAGE-team*, 2001]. These higher temperatures from *Leemans et al.* [2002] relative to the present study are further amplified by positive feedbacks in the climate-carbon cycle system, with relative enhancements in soil respiration and Ocean outgassing of CO_2 at higher temperatures. A recent study using the HadCM3 climate model [*Johns et al.*, 2003], including future sulfur emissions, project future increases in global temperature of $1.9^\circ C$ (B1), $2.2^\circ C$ (B2), and $3.1^\circ C$ (A2). Although in better agreement with *Johns et al.* [2003], the present study does not consider the cooling effect of future sulfate aerosol emissions, and therefore should be considered in the lower range of published estimates.

[57] The future impact of land cover change on absolute global and regional temperatures is similar for A2 and B1. However, underlying these similar net responses are marked differences in the biogeophysical and biogeochemical effects among scenarios. In relative terms, the contribution of land cover changes to future temperature changes range between 9% (A1B) and 16% (B2) with intermediate values of 10% and 13% for A2 and B1, respectively. Despite the maximum contribution of land cover changes to atmospheric CO_2 (22%) in A2, owing to the most extensive tropical and subtropical deforestation among scenarios, the associated biogeophysical cooling results in land cover changes contributing only 10% to future warming, the second lowest among scenarios. In contrast, for B1, biogeophysical warming associated with temperate forest regrowth amplifies the biogeochemical effect; hence land cover changes contribute more to future temperature increases (13%) than to atmospheric CO_2 (9%). In B1, the biogeophysical warming effect, due to temperate reforestation, is of similar magnitude and the same sign as the biogeochemical warming caused by low-latitude deforestation. A climate warming resulting from mid- to high-latitude reforestation is in agreement with findings of *Betts* [2000]. In A2 the impact of large-scale tropical and subtropical land conversion is a large biogeochemical warming opposed by a smaller biogeophysical cooling. This biogeophysical cooling is in fact not in contradiction to the findings of *DeFries et al.* [2002]. They ran the CSU GCM with a future land cover data set for year 2050 from IMAGE 2.1 and sea surface temperatures (SST) prescribed from present-day observations. *DeFries et al.* [2002] show that in the tropics, reduced plant productivity leads to a reduction in ratio of latent to sensible heat flux, inducing seasonal surface warming (up to $2^\circ C$) and

drying. CLIMBER-2 simulations with tropical deforestation show surface warming in the case of prescribed ocean SSTs, but reveal a global-scale cooling with interactive ocean SSTs and sea ice [*Ganopolski et al.*, 2001]. Additional simulations with fixed ocean SSTs (not shown) for A2 and B1 confirm this point. Because of the coarse spatial resolution of CLIMBER-2, the simulated climate changes within the continental interiors, with fixed SSTs, are not as pronounced as in models with finer resolution.

[58] *House et al.* [2002] estimated complete deforestation to increase atmospheric CO_2 concentrations by 130–290 ppmv. In this study the difference in atmospheric CO_2 between complete future deforestation (1288 ppm) and reforestation (806 ppm) for scenario A2 is considerably larger at 482 ppm, comparable to the range associated with uncertainties in fossil fuel CO_2 emissions alone (258 ppm). This range increases to 736 ppm when for illustration the lowest (B1) and highest (A2) fossil fuel CO_2 emission scenarios are completely reforested and deforested, respectively, by 2100. Given this uncertainty, further attention is warranted to improve projections of future societal-economic development.

[59] For complete future deforestation, in both A2 and B1 the land biosphere is projected to become a future source of carbon, releasing up to 13–14 PgC/yr by year 2100 (Figure 9). Given the linear scenario of deforestation applied, a constant land source over the whole period may be expected. However, land carbon dynamics are nonlinear, owing to the lagged response of soil carbon and product pool decomposition and the cumulative CO_2 fertilization effect, many years after the initial land cover perturbation. A cumulative land release of 787 PgC for complete deforestation is larger than estimates of 270–610 PgC from *House et al.* [2002], which explains the higher atmospheric CO_2 levels attributed to deforestation in the current study. LPJ estimates larger present-day biomass stocks than those used by *House et al.* [2002], and the latter study did not consider the transient impacts of increased CO_2 on future vegetation biomass.

[60] Similarly, for future reforestation A2min the current study estimates a cumulative CO_2 uptake of 382 PgC, larger than the 200 PgC assumed by *House et al.* [2002]. The latter is in fact an estimate of the cumulative historical land use flux, and with reforestation the land biosphere is assumed to uptake a similar amount. Again, transient effects of increased atmospheric CO_2, climate, and their synergy on plant production and biomass were not considered. Reforestation reduces atmospheric CO_2 by ~24 ppm in the current study, compared with 40–70 ppm from *House et al.* [2002]. However, these estimates are not directly comparable because the temporal dynamics of the flux may be different, and this affects atmospheric CO_2. Reforestation scenarios show greater net land uptake than in baseline scenarios. Indeed, in A2 the trend toward land release is reversed in the reforestation scenario, becoming a large net land uptake up to ~5 PgC/yr by 2100.

5. Conclusions

[61] This study combines for the first time a consistent set of fossil fuel CO_2 emission scenarios and geographically explicit land cover change maps used to drive CLIMBER2-LPJ, a climate–carbon cycle model including dynamic vegetation and biogeophysical feedbacks. Results indicate that with interactive land cover change simulated atmospheric CO_2 could be higher than previously reported. This is due to the inclusion of the biogeophysical effect of land cover change in CLIMBER2-LPJ, differences in parameterizations of hydrological and biogeochemical processes, and likely differences in initial biomass and carbon pools. Despite inclusion of fluxes associated with land cover changes, results show cumulative net land uptake for all four baseline SRES scenarios.

[62] The relative role of land cover changes in atmospheric CO_2 growth represents 9–22%, the remainder attributable to fossil fuel CO_2 emissions. This represents a decrease in comparison with the 18% average relative role for the period 1960–1990 [*Brovkin et al.*, 2004]. Differences in the relative contribution of land cover change to atmospheric CO_2 and temperature for individual scenarios highlight the importance of considering both biogeophysics and biogeochemistry in impact studies of future land cover changes on climate and its composition. For example, in A2, land cover changes contribute 22% to CO_2, but only 10% to future temperature.

[63] Biogeophysical effects of land cover change vary in both sign and magnitude depending on the location and extent of land conversion and abandonment. Extensive tropical and subtropical deforestation in A2 and less extensive tropical conversion combined with temperate land abandonment in B1 lead to a biogeophysical cooling and warming, respectively. In A2, biogeophysical cooling reduces the larger biogeochemical warming associated with tropical deforestation. Consequently, temperature growth in A2 is lower than previously reported by *Joos et al.* [2001], despite higher CO_2 levels, although some difference might be due to the different climatic forcings accounted for by *Joos et al.* [2001]. For both A2 and B1, the net effect of land cover changes is similar, with a warming of $0°–0.25°C$ in the tropics and subtropics and between $0.25°C$ and $0.5°C$ and above at higher latitudes.

[64] In hypothetical experiments with complete deforestation and reforestation, results show a range of uncertainty in atmospheric CO_2 double to that associated with choice of fossil fuel CO_2 emission scenario. Nevertheless, given that CLIMBER-2 has a moderate climate sensitivity of $2.5°C/2xCO_2$, these estimates of future atmosphere CO_2 concentration and temperature change should be considered as conservative.

References

Betts, R. A. (2000), Offset of the potential carbon sink from boreal forestation by decreases in surface albedo, *Nature*, *408*, 187–190.

Betts, A. K., and J. H. Ball (1997), Albedo over the boreal forest, *J. Geophys. Res.*, *102*, 28,901–28,909.

Brovkin, V., A. Ganopolski, and Y. Svirezhev (1997), A continuous climate-vegetation classification for use in climate-biosphere studies, *Ecol. Modell.*, *101*, 251–261.

Brovkin, V., A. Ganopolski, M. Claussen, C. Kubatzki, and V. Petoukhov (1999), Modelling climate response to historical land cover change, *Global Ecol. Biogeogr.*, *8*, 509–517.

Brovkin, V., J. Bendtsen, M. Claussen, A. Ganopolski, C. Kubatzki, V. Petoukhov, and A. Andreev (2002), Carbon cycle, vegetation and climate dynamics in the Holocene: Experiments with the CLIMBER-2 model, *Global Biogeochem. Cycles*, 16(4), 1139, doi:10.1029/2001GB001662.

Brovkin, V., S. Sitch, W. von Bloh, M. Claussen, E. Bauer, and W. Cramer (2004), Role of land cover changes for atmospheric CO_2 increase and climate change during the last 150 years, *Global Change Biol.*, 10, 1–14, doi:10.1111/j.1365-2486.2004.00812.x.

Claussen, M., V. Brovkin, A. Ganopolski, C. Kubatzki, V. Petoukhov, and S. Rahmstorf (1999), A new model for climate system analysis: Outline of the model and application to palaeoclimate simulations, *Environ. Model. Assess.*, 4, 209–216.

Claussen, M., V. Brovkin, and A. Ganopolski (2001), Biogeophysical versus biogeochemical feedbacks of large-scale land cover change, *Geophys. Res. Lett.*, 28(6), 1011–1014.

Cox, P. M., R. A. Betts, C. D. Jones, S. A. Spall, and I. J. Totterdell (2000), Acceleration of global warming due to carbon-cycle feedbacks in a coupled climate model, *Nature*, 408, 184–187.

Cramer, W., et al. (2001), Global response of terrestrial ecosystem structure and function to CO_2 and climate change: Results from six dynamic global vegetation models, *Global Change Biol.*, 7, 357–373.

Cramer, W., A. Bondeau, S. Schaphoff, W. Lucht, B. Smith, and S. Sitch (2004), Tropical forests and the global carbon cycle: Impacts of atmospheric CO_2, climate change and rater of deforestation, *Philos. Trans. R. Soc. London, Ser. B*, 359, 331–343, doi:10.1098/rstb.2003.1428.

Cubasch, U., G. A. Meehl, G. J. Boer, R. J. Stouffer, M. Dix, A. Noda, C. A. Senior, S. Raper, and K. S. Yap (2001), Projections of future climate change, in *Climate Change 2001: The Scientific Basis—Contribution of Working Group I to the Third Assessment Report of the Intergovernmental Panel on Climate Change*, 1st ed., edited by J. T. Houghton et al., pp. 527–582, Cambridge Univ. Press, New York.

Defries, R. S., L. Bounoua, and G. J. Collatz (2002), Human modification of the landscape and surface climate in the next fifty years, *Global Change Biol.*, 8, 438–458.

Dufresne, J.-L., P. Friedlingstein, M. Berthelot, L. Bopp, P. Ciais, L. Fairhead, H. Le Treut, and P. Monfray (2002), On the magnitude of positive feedback between future climate change and the carbon cycle, *Geophys. Res. Lett.*, 29(10), 1405, doi:10.1029/2001GL013777.

Friedlingstein, P., L. Bopp, P. Ciais, J.-L. Dufresne, L. Fairhead, H. Le Treut, P. Monfray, and J. Orr (2001), Positive feedback between future climate change and the carbon cycle, *Geophys. Res. Lett.*, 28, 1543–1546.

Ganopolski, A., V. Petoukhov, S. Rahmstorf, V. Brovkin, M. Claussen, A. Eliseev, and C. Kubatzki (2001), CLIMBER-2: A climate system model of intermediate complexity: II. Validation and sensitivity tests, *Clim. Dyn.*, 17(10), 735–751, doi:10.1007/s003820000144.

Gitz, V., and P. Ciais (2003), Amplifying effects of land-use change on future atmospheric CO_2 levels, *Global Biogeochem. Cycles*, 17(1), 1024, doi:10.1029/2002GB001963.

Houghton, R. A. (2003), Revised estimates of the annual net flux of carbon to the atmosphere from changes in land use and land management 1850–2000, *Tellus, Ser. B*, 55, 378–390.

House, J. I., I. C. Prentice, and C. Lequéré (2002), Maximum impacts of future reforestation or deforestation on atmospheric CO_2, *Global Change Biol.*, 8, 1047–1052.

IMAGE-team (2001), *The IMAGE 2.2 Implementation of the SRES scenarios: A Comprehensive Analysis of Emissions, Climate Change and Impact in the 21st Century* [CD-ROM], *RIVM Publ. 481508018*, Natl. Inst. of Public Health and the Environ. (RIVM), Bilthoven, Netherlands.

Johns, T. C., et al. (2003), Anthropogenic climate change for 1860 to 2100 simulated with the HadCM3 model under updated emissions scenarios, *Clim. Dyn.*, 20, 583–612.

Jones, C. J., P. M. Cox, R. L. H. Essery, D. L. Roberts, and M. J. Woodage (2003a), Strong carbon cycle feedbacks in a climate model with interactive CO_2 and sulphate aerosols, *Geophys. Res. Lett.*, 30(9), 1479, doi:10.1029/2003GL016867.

Jones, C. J., P. Cox, and C. Huntingford (2003b), Uncertainty in climate-carbon-cycle projections associated with the sensitivity of soil respiration to temperature, *Tellus, Ser. B*, 55, 642–648.

Joos, F., I. C. Prentice, S. Sitch, R. Meyer, G. Hooss, G.-K. Plattner, S. Gerber, and K. Hasselmann (2001), Global warming feedbacks on terrestrial carbon uptake under the Intergovernmental Panel on Climate Change (IPCC) emission scenarios, *Global Biogeochem. Cycles*, 15(4), 891–907.

Leemans, R., B. Eickhout, B. Strengers, L. Bouwman, and M. Schaeffer (2002), The consequences of uncertainties in land use, climate and vegetation responses on the terrestrial carbon, *Sci. China*, 45, 17 pp.

Matthews, H. D., A. J. Weaver, M. Eby, and K. J. Meissner (2003), Radiative forcing of climate by historical land cover change, *Geophys. Res. Lett.*, 30(2), 1055, doi:10.1029/2002GL016098.

Matthews, H. D., A. J. Weaver, K. J. Meissner, N. P. Gillett, and M. Eby (2004), Natural and anthropogenic climate change: Incorporating historical land cover change, vegetation dynamics and the global carbon cycle, *Clim. Dyn.*, 22, 461–479, doi:10.1007/s00382-004-0392-2.

McGuire, A. D., et al. (2001), Carbon balance of the terrestrial biosphere in the twentieth century: Analyses of CO_2, climate and land use effects with four process-based ecosystem models, *Global Biogeochem. Cycles*, 15(1), 183–206.

Morita, T., et al. (2001), Greenhouse gas emission mitigation scenarios and implications, in *Climate Change 2001: Mitigation—Contribution of Working Group III to the Third Assessment Report of the Intergovernmental Panel on Climate Change*, pp. 115–166, Cambridge Univ. Press, New York.

Nakićenović, N., et al. (2000), *Special Report on Emission Scenarios*, Cambridge Univ. Press, New York.

New, M., M. Hulme, and P. D. Jones (1999), Representing twentieth-century space-time climate variability: I. Development of a 1961–90 mean monthly terrestrial climatology, *J. Clim.*, 12, 829–856.

New, M., M. Hulme, and P. D. Jones (2000), Representing twentieth-century space-time climate variability: II. Development of 1901–96 monthly grids of terrestrial surface climate, *J. Clim.*, 13, 2217–2238.

Petoukhov, V., A. Ganopolski, V. Brovkin, M. Claussen, A. Eliseev, C. Kubatzki, and S. Rahmstorf (2000), CLIMBER-2: A climate system model of intermediate complexity: I. Model description and performance for present climate, *Clim. Dyn.*, 16, 1–17.

Prentice, I. C., G. D. Farquhar, M. J. R. Fasham, M. L. Goulden, M. Heimann, V. J. Jaramillo, H. S. Kheshgi, C. Le Quéré, R. J. Scholes, and D. W. R. Wallace (2001), The carbon cycle and atmospheric carbon dioxide, in *Climate Change 2001: The Scientific Basis—Contribution of Working Group I to the Third Assessment Report of the Intergovernmental Panel on Climate Change*, 1st ed., edited by J. T. Houghton et al., pp. 185–225, Cambridge Univ. Press, New York.

Ramankutty, N., and J. A. Foley (1999), Estimating historical changes in global land cover: Croplands from 1700 to 1992, *Global Biogeochem. Cycles*, 13(4), 997–1027.

Schimel, D., et al. (1996), Radiative forcing of climate change, in *Climate Change 1995: The Science of Climate Change*, edited by J. T. Houghton et al., chap 2, pp. 65–131, Cambridge Univ. Press, New York.

Sitch, S., et al. (2003), Evaluation of ecosystem dynamics, plant geography and terrestrial carbon cycling in the LPJ dynamic global vegetation model, *Global Change Biol.*, 9, 161–185.

Vitousek, P. M., H. A. Mooney, J. Lubchenco, and J. M. Melillo (1997), Human domination of Earth's ecosystems, *Science*, 277, 494–499.

Wigley, T. M. L., A. K. Jain, F. Joos, B. S. Nyenzi, and P. R. Shukla (1997), Implications of proposed CO_2 emissions limitations, *Tech. Pap. 4*, edited by J. T. Houghton et al., 41 pp., Intergov. Panel on Clim. Change, Bracknell, UK.

————————————

V. Brovkin, A. Ganopolski, and W. von Bloh, Potsdam Institute for Climate Impact Research, Potsdam, Germany.

B. Eickhout and D. van Vuuren, Netherlands Environmental Assessment Agency (RIVM/MNP), Bilthoven, Netherlands.

S. Sitch, Met Office (JCHMR), Maclean Building, Crowmarsh-Gifford, Wallingford, OX10 8BB, UK. (stephen.sitch@metoffice.com)
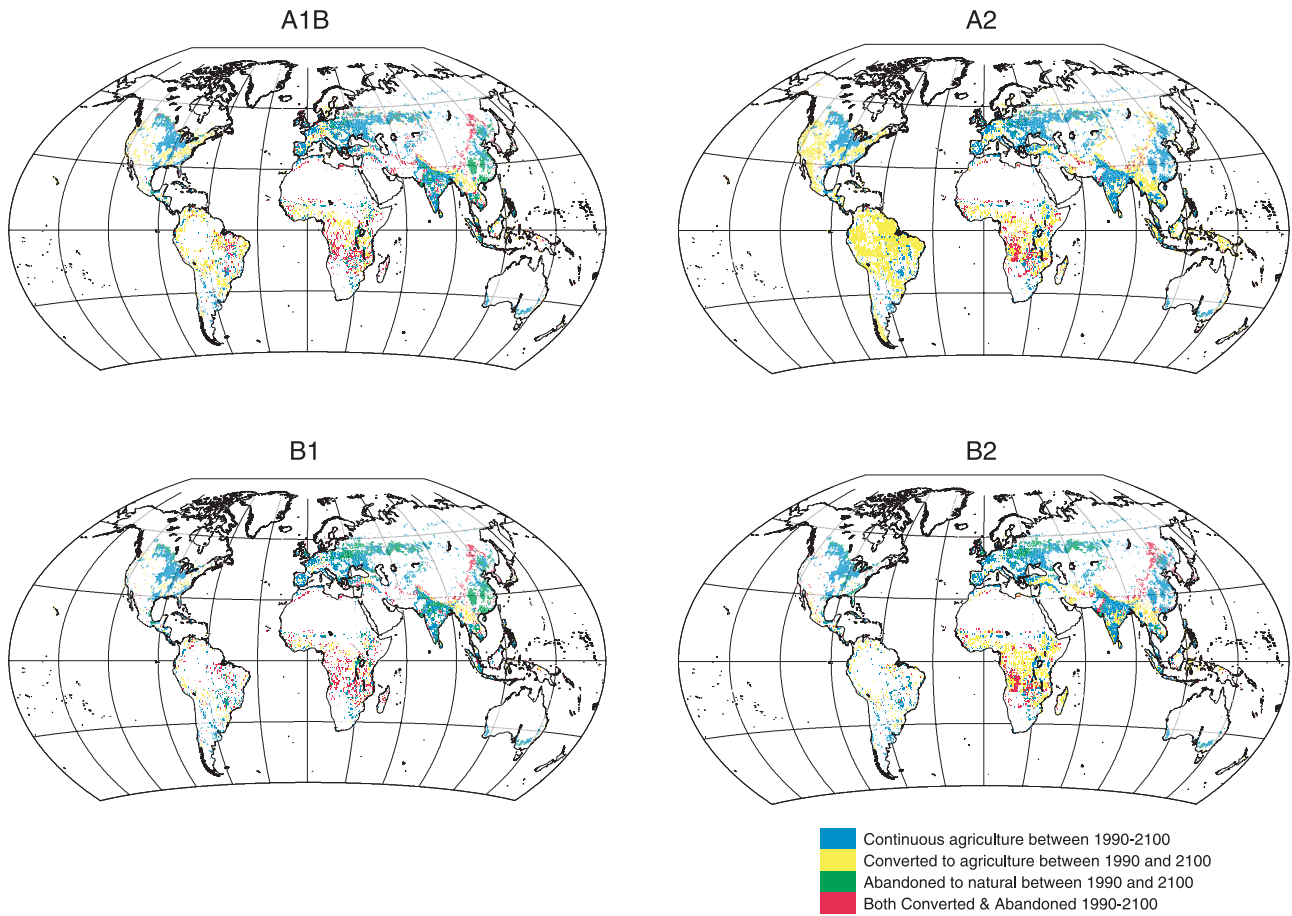
Figure 3. Geographically explicit IMAGE 2.2 land cover changes, 1990–2100, for four SRES scenarios; anomaly approach to RF historical cropland data set.
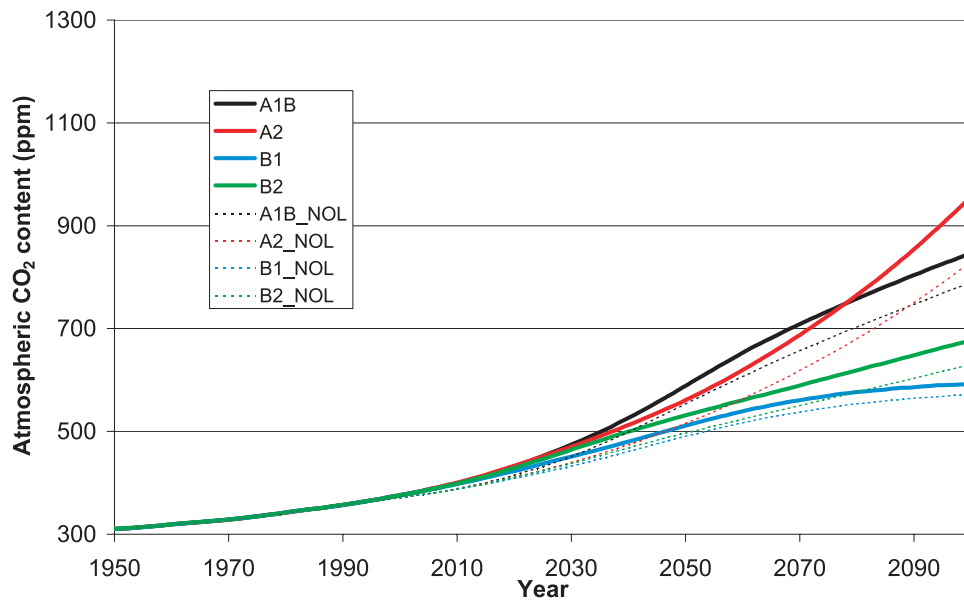
Figure 4. Atmospheric CO_2 concentrations 1950–2100 for four SRES scenarios, and simulations with no land cover changes after 2000.
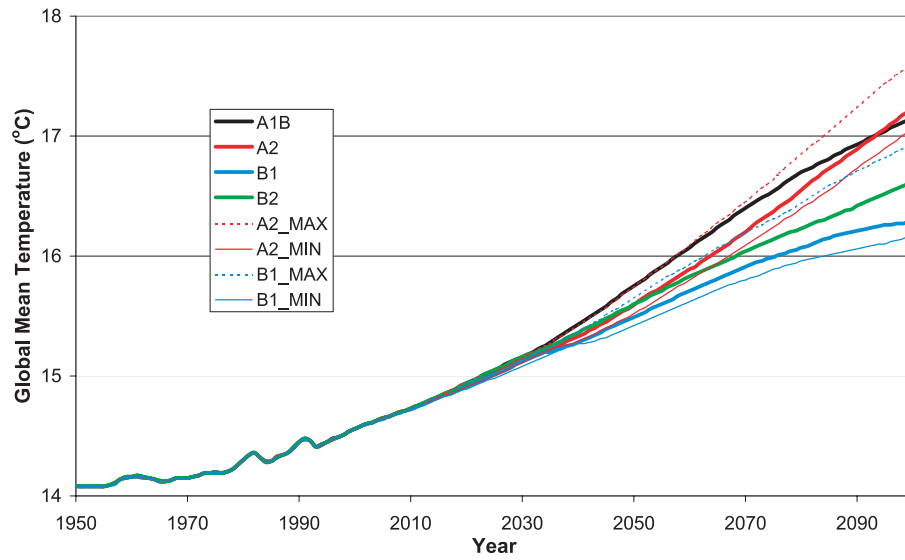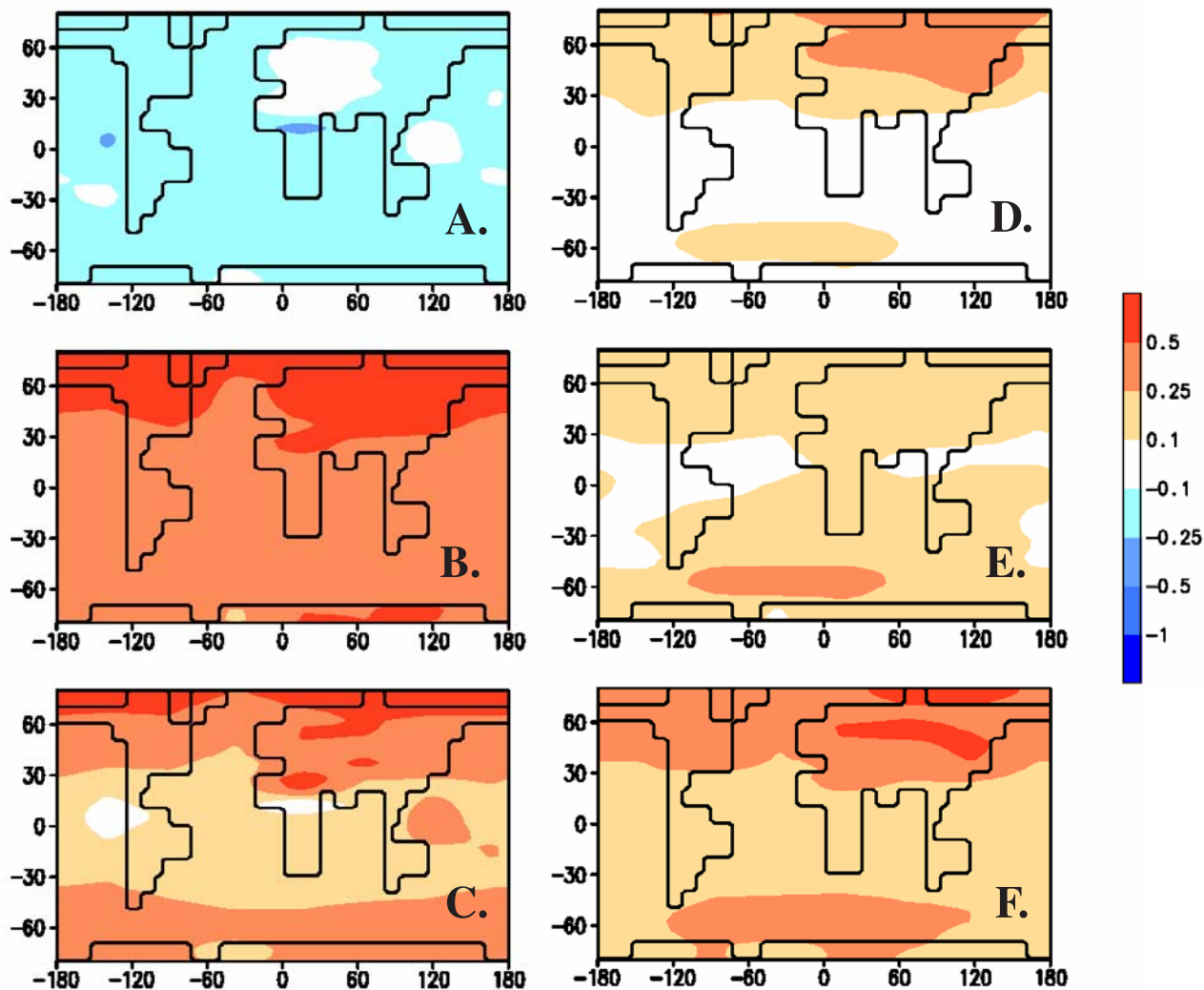
Figure 5. Global mean annual temperature for the four SRES scenarios.

Figure 6. Simulated changes in mean annual temperature (°C) due to land cover changes only. (a) A2 biogeophysical effect (A2phys-A2_nol), (b) A2 biogeochemical effect (A2chem-A2_nol), (c) A2 net effect (A2-A2_nol), (d) B1 biogeophysical effect (B1phys-B1_nol), (e) B1 biogeochemical effect (B1chem-B1_nol), and (f) B1 net effect (B1-B1_nol).

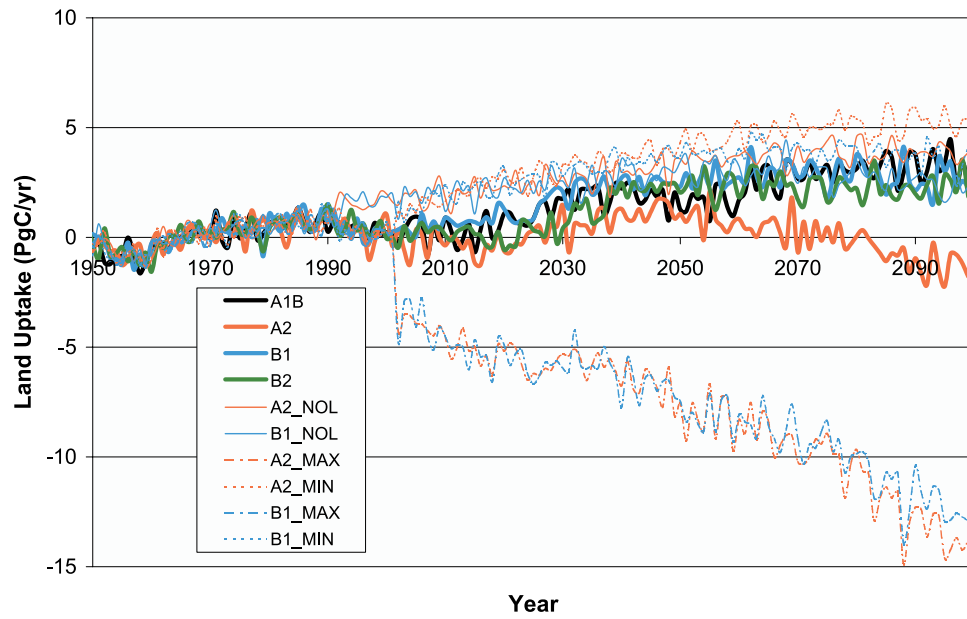**Figure 9.** Net land uptake for four SRES scenarios.